Computational Materials Science 129 (2017) 273–278

Contents lists available at ScienceDirect

Computational Materials Science

journal homepage: www.elsevier.com/locate/commatsci

Influence of surface atomic structure on the mechanical response of aluminum nanospheres under compression

S. Bel Haj Salah, C. Gerard, L. Pizzagalli *

Institut Pprime - CNRS UPR3346, Université de Poitiers - CNRS - ISAE-ENSMA, F86962 Chasseneuil Futuroscope Cedex, France

ARTICLE INFO

Article history:
Received 31 August 2016
Received in revised form 21 December 2016
Accepted 23 December 2016
Available online 10 January 2017

Keywords:
Nanoparticle
Plasticity
Dislocations
Molecular dynamics
Aluminum

ABSTRACT

Molecular Dynamic simulations have been performed to study the mechanical behavior of ⟨1 0 0⟩ oriented aluminum nanospheres under compression, and the influence of size on plasticity mechanisms and yield stress. Plasticity always started by the nucleation of partial dislocations from the surface contact edges. For large enough nanoparticles, the formation of pyramidal structures is observed in a pseudo-elastic regime. The pyramid apex favors dislocation nucleation at high compression levels. The plasticity mechanisms and the yield stress do not depend on nanoparticle size. Instead, our results suggest that the geometry and atomic structure of the layers in contact with the indenters control the plastic deformation.

1. Introduction

Compared to bulk materials, nano-objects such as nanowires or nanoparticles often exhibit drastically different mechanical properties (e.g., hardness, elastic moduli, toughness, etc.) and in particular a strong dependence on size [1–5]. As a consequence, an intense research effort has been made to characterize the mechanical behavior of low dimension systems for the last decade [6,7].

The interest for a better understanding of the plastic deformation of nanoparticles also increased recently, but the corresponding literature remains limited, noticeably because of the difficulties associated to the experimental mechanical testing. Gerberich et al. provided one of the first observations in the matter, by performing axial compression on gold and silicon nanospheres, and using transmission electron microscopy to characterize the plastic deformation [1,8–11]. Theoretically, molecular dynamic studies were performed for silicon nanospheres [12,13], gold [5] and α-iron [14] faceted nanoparticles. In particular, Mordehai et al. reported that a dislocations nucleation process occurs from the surface in gold nanoparticles, in agreement with the mechanism proposed by Gerberich for silicon nanospheres [1,11]. These dislocations annihilate on the lateral surfaces of the faceted particles, leading then to defect-free particles during indentation [5]. On the contrary, dislocations remain pinned to the nucleation site for α-iron metallic nanoparticles [14].

The shape of the nanoparticle is also expected to play a role. For instance, the dislocation nucleation of Ni_3Al nanocubes under uniaxial compression was recently simulated [15,16]. The nucleation of the first Shockley partial dislocations is reported from the edge or the vertices of the cube, followed by a pseudo-twinning process. However, the nucleation from the edge or the vertices may be related to the idealized shape of the cube, since real Ni_3Al cubic nanoprecipitates exhibit rounded edge and vertices [17].

At last, Bian and Wang [18] performed molecular dynamics simulations of a copper nanosphere compressed along the [001] crystalline direction, and described the nucleation dislocation process. Though this description is limited to the case of a 20 nm nanoparticle, this work revealed how the nucleation of Shockley dislocations occurred at the contact edges between the nanosphere and the flat indenter. These Shockley dislocations propagate and intersect to form two successive dislocation pyramidal structures.

It is noteworthy that this last study was limited to a single size for the copper nanospheres. It is highly desirable to investigate whether this plasticity mechanism is not specific, and to characterize an eventual size influence on plasticity mechanisms and yield stress. We thus report in this paper a detailed description of the plastic deformation of an aluminum spherical nanoparticle, with a focus on the nanoparticle size influence in the range 4–20 nm.

2. Simulation method

In this study, molecular dynamics simulations were performed using the Large-Scale Atomic/Molecular Massively Parallel Simula-

* Corresponding author.
E-mail address: laurent.pizzagalli@univ-poitiers.fr (L. Pizzagalli).

http://dx.doi.org/10.1016/j.commatsci.2016.12.033
0927-0256/

tor code, LAMMPS [19]. For the interatomic interactions, we used the embedded-atom method potential developed by Mishin et al. [20,21], yielding a lattice constant $a_0 = 4.05$ Å for aluminum. This potential accurately represents dislocations and in particular their nucleation and propagation [22–24].

Monocrystalline spherical nanoparticles were initially built by carving a sphere out of bulk with a given diameter ø, taking care that top and bottom surfaces along [0 1 0] orientation were rigorously identical. We also selected diameter values yielding well defined facets, in order to avoid unrealistic contact surfaces made of few atoms. Each system was first relaxed to a local energy minimum using conjugate gradients, then the nanoparticle was thermally equilibrated by molecular dynamics in the NVT ensemble with a timestep of 1 fs, and at a temperature of 10 K using a Nose-Hoover thermostat [25]. This step leads to a negligible volume variations of nanospheres, suggesting a very weak relaxation associated with surfaces creation and the quasi-absence of hydrostatic pressure inside the spheres before mechanical deformation. The separation d_0 between top and bottom (0 1 0) surfaces, after relaxation, corresponds to the reference state at the beginning of the compression test. d_0 values for each nanoparticle are reported in Table 1. Note that these values are typically lower than the corresponding diameters used to build the nanoparticle because of the discrete character of atomic systems.

In order to perform the uniaxial compression, each particle was placed between two planar repulsive force fields, perpendicular to the [0 1 0] crystal axis of the nanoparticle, as shown in Fig. 1. Experimentally, the compression is usually carried out using indenters whose the curvature is large enough compared to the nanosphere so that the mechanical sollication is equivalent to an axial compression. In simulations, those can then be modeled by using a planar repulsive force field [12,18]. The external forces acting on a nanosphere atom are computed according to a chosen analytical function and to the separation between the planar force field and atom position as given by:

$$F_y(y) = -\alpha k(y - y_i)^2 \quad (1)$$

where y_i is the position of indenter along [0 1 0], y is the coordinate for that atom along the same axis and k is a constant related to the effective stiffness of the indenter, which has been fixed to 1000 eV Å^{-3} in our study. For the top indenter $\alpha = 1$ when $y \geqslant y_i$ and $\alpha = 0$ when $y < y_i$, while for the bottom indenter, $\alpha = -1$ when $y \leqslant y_i$ and $\alpha = 0$ when $y > y_i$. Initially, indenters are located at the same positions than (0 1 0) nanoparticle surfaces. Then both indenters were moved towards the particle with a strain rate of 10^9 s^{-1}, at 10 K. Tests performed at a lower rate of 10^8 s^{-1} showed no appreciable differences. No periodic boundary conditions were used in any dimension of the simulation box. The compression depth is $\delta = d_0 - d$, with d the [0 1 0] distance between indenters during compression. At each deformation step, we computed the contact surface area between the nanosphere and the indenter according to the following procedure: (i) a nanosphere atom is considered to belong to the contact surface if $|y - y_i| < 0.1$ Å (ii) the total contact area is computed following the method proposed by Vergeles et al. [26].

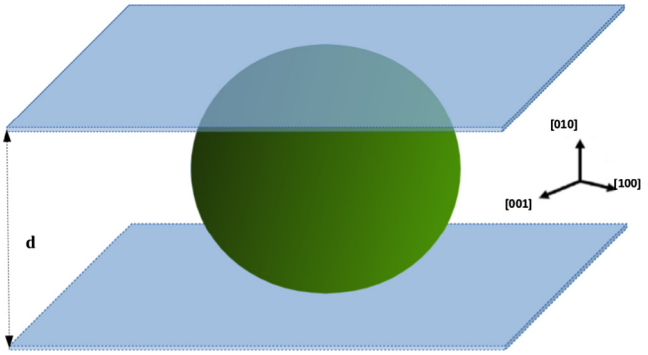

Fig. 1. Compression setup of a nanosphere.

Dislocations and defect structures were analyzed using coordination numbers [27] and the central symmetry parameter [28]. Molecular dynamics data were analyzed and visualized using the packages Ovito [29] and ParaView [30].

3. Results

3.1. Plastic deformation mechanisms

We first describe the compression test, using as an illustrative example the case of a 20.01 nm nanoparticle. At the beginning, an elastic behavior is obtained, as can be seen on the stress vs deformation curves in the Fig. 2. The first evidence of plastic deformation occurs at a compression depth $\delta = 5.46$ Å (i.e. 2.75% deformation), when eight Shockley partial dislocations are emitted from the top and bottom contact surface edges of the nanosphere (four from the top and four from the bottom), and propagate in the four possible {1 1 1} slip planes, as shown in Fig. 3(a), yielding the small stress drop in Fig. 2.

We found that in all considered nanoparticles, the initiation of plasticity is due to the nucleation of these partial dislocation from the edges of the surface in contact with indenters. The edges actually form steps with the underneath layer and act as stress concentrators, a phenomenon well established in the case of the uniaxial deformation of surfaces [22]. At the yield stress, the maximum atomic shear stress values are about 4 GPa, and are associated with atoms on both sides of the {1 1 1} planes emerging at the base of steps.

When $\delta = 5.6$ Å (2.82%), atomic layers at top and bottom, forming the initial contact surfaces, merge with their respective underneath layers. The intersection of the Shockley partial dislocations (Fig. 3(b)) forms four stair-rod $\frac{1}{3}[1\,0\,0]$ dislocations according to the reaction:

$$\frac{1}{6}[1\,1\,\bar{2}] + \frac{1}{6}[1\,\bar{1}\,2] = \frac{1}{3}[1\,0\,0]. \quad (2)$$

These stair-rod dislocations constitute a pyramid-like structure (Fig. 3(c)), that has already been observed for another system [18]. As the compression continues, new partial Shockley dislocations are nucleated from the new contact surface edges, as shown in

Table 1
Data characterizing the nanoparticle structure (see text and Fig. 5 for the definition of ø, d_0, λ_1 and λ_2), the first nucleated dislocation (load, contact surface S, and yield stress σ_1^c), and the first nucleated dislocation from the pyramid apex (σ_2^c).

ø (nm)	d_0 (nm)	λ_1 ($\sqrt{2}a_0/4$)	λ_2 ($\sqrt{2}a_0/4$)	Load (nN)	S (nm^2)	σ_1^c (GPa)	σ_2^c (GPa)
4.01	3.65	3	1	31.4	2.5	12.46	
8.00	7.70	3	3	50.6	4.1	12.47	10.60
20.01	19.83	9	5	58.8	4.7	12.49	10.02
20.17	19.84	7	5	101.1	9.4	10.74	11.76

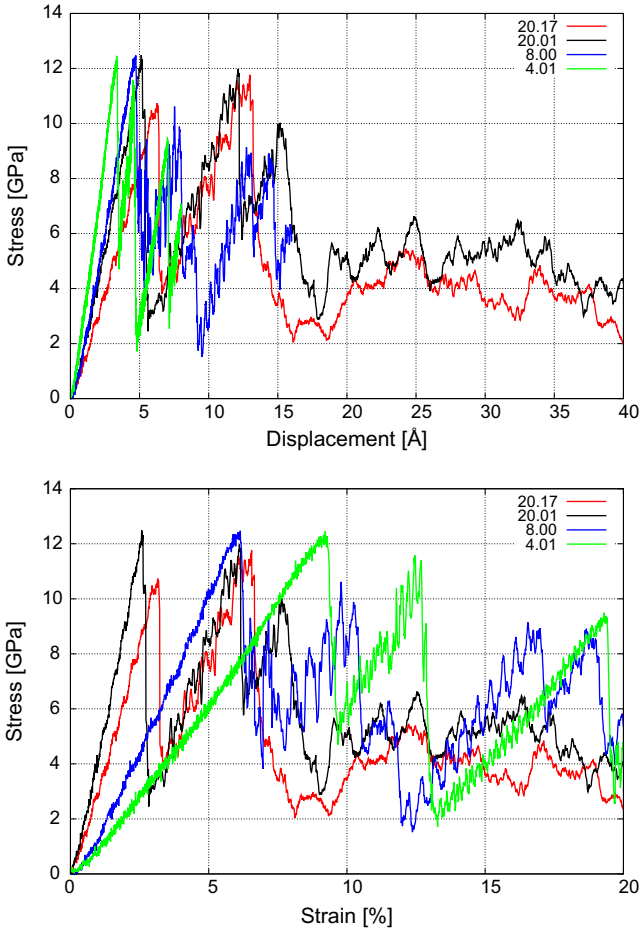

Fig. 2. Contact stress as a function of displacement (top graph) and strain (bottom graph) for the investigated nanospheres.

Fig. 3(d). Again, those partial dislocations propagate and intersect, as marked by red arrows in Fig. 3(f), to form a second pyramid, larger than the first one. When $\delta = 12.36$ Å (6.23%), the second atomic layer is merged with the third one, see Fig. 3(g). During compression we also observe the formation a $\frac{1}{3}[\bar{1}01]$ stair-rod dislocation, from the intersection between two $\frac{1}{3}<100>$ stair-rod dislocations (blue arrow on Fig. 3(h)), according to:

$$\frac{1}{3}[\bar{1}00]+\frac{1}{3}[001]=\frac{1}{3}[\bar{1}01]. \quad (3)$$

However, the initial pyramidal structure is recovered when compression increases. Note that this double pyramid configuration is obtained for both top and bottom contact surfaces. Starting from this defected structure, simulations were performed in which the load is progressively reversed. We found that the partial dislocations loops forming the pyramidal-like structures progressively retract towards the contact surface, leading to the complete recovery of the pristine nanosphere structure.

Now considering again the double pyramid configuration, and increasing δ to 15.18 Å (7.65%), one $\frac{1}{3}[100]$ stair-rod dislocation in the larger pyramid begins to dissociate into two Shockley partial dislocations (Fig. 3(j)). Then, these partial dislocations, with one end contacting the surface and the other pinned at the tip of the pyramid, expand (Fig. 3(k, l)). This corresponds to the large load drops that can be seen for the largest nanoparticles at about 6.5% and 7.5% in Fig. 2.

As the compression continues, Shockley partial dislocations, separated by an intrinsic stacking fault, are nucleated from the dissociation of the larger pyramid edges and propagate through the nanoparticle (4(a, b)). The resulting plastic deformation is now conserved if the load is removed, in contrast to the pyramidal-like structure formation, which may be considered as a pseudo-elastic regime. These dislocations interact and form other dislocations like stair-rod dislocation with Burgers vectors $\frac{1}{3}<100>$, stair-rod dislocation with Burgers vectors $\frac{1}{6}<1\bar{1}0>$, and perfect dislocations with Burgers vectors $\frac{1}{2}<110>$ (marked respectively by red, orange and light blue arrows in Fig. 4(c, d)). But these dislocation segments remain short and disappear upon further compression. Shockley partial dislocation then glide through the nanoparticle and annihilate at opposite surfaces. This nucleation expansion mechanism is observed until the largest compression depth investigated here ($\delta = 36.86$ Å, 18.6%), and progressively deconstructs the pyramidal structures on both contact surfaces.

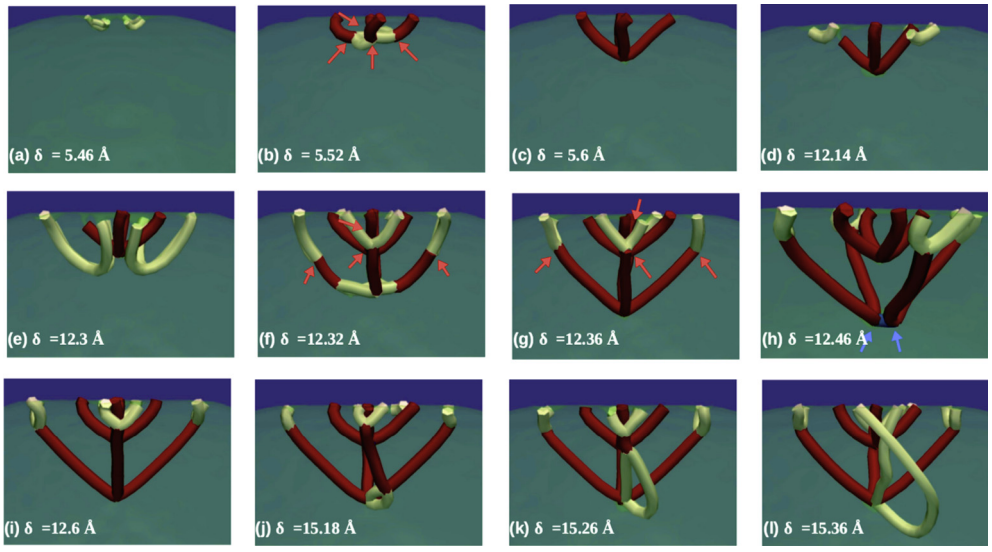

Fig. 3. Dislocation structures occurring during the uniaxial compression of a 20.01 nm Al nanosphere at 10 K (white line, Shockley partial dislocation with Burgers vectors $\frac{1}{6}<112>$; red line, stair-rod dislocation with Burgers vectors $\frac{1}{3}<100>$ and blue line, stair-rod dislocation with Burgers vectors $\frac{1}{3}<110>$). (For interpretation of the references to colour in this figure legend, the reader is referred to the web version of this article.)

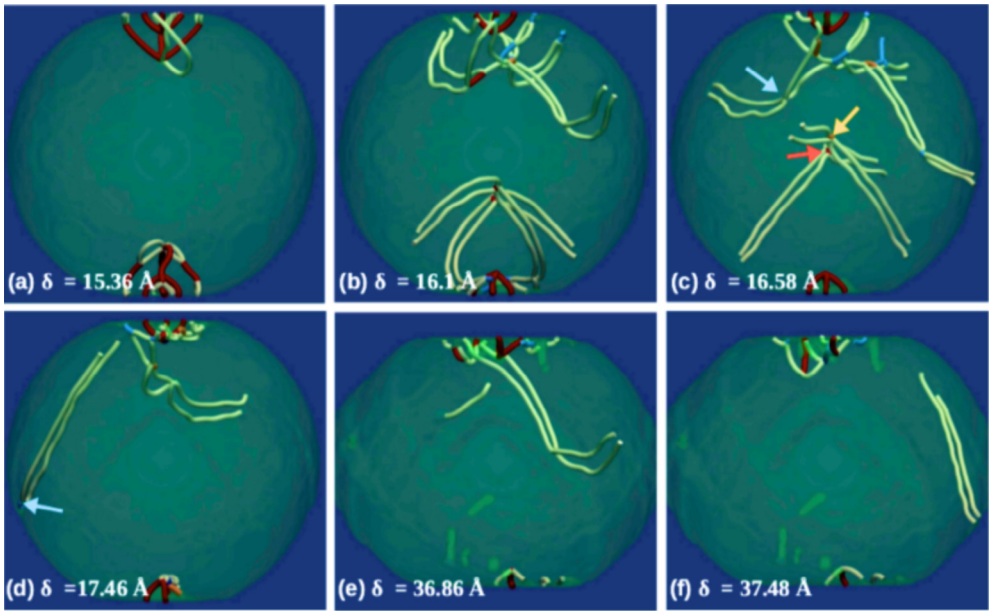

Fig. 4. Dislocation structures occurring during the uniaxial compression of a 20.01 nm Al nanosphere at 10 K (white line, Shockley partial dislocation with Burgers vectors $\frac{1}{6}<1\,1\,2>$; red line, stair-rod dislocation with Burgers vectors $\frac{1}{3}<1\,0\,0>$; orange line, stair-rod dislocation with Burgers vectors $\frac{1}{6}<1\,\bar{1}\,0>$; blue sky, perfect dislocation with Burgers vectors $\frac{1}{2}<1\,1\,0>$). (For interpretation of the references to colour in this figure legend, the reader is referred to the web version of this article.)

3.2. Size effect

We now discuss the variations in plasticity mechanisms observed for the other nanoparticle sizes, with respect to the previous scenario. Considering a smaller 8.00 nm nanosphere, the first evidence of plastic deformation occurs at a compression depth $\delta = 4.68$ Å (6.1%), thus at a greater strain than for the larger nanoparticle. Nevertheless, the plasticity mechanisms are relatively similar, i.e. partial dislocations are nucleated from the surface contact edges. These partial dislocations propagate until the first pyramid structure is formed at $\delta = 4.76$ Å (6.2%). However, unlike the larger nanoparticle, increasing the compression does not lead to the nucleation of new partial dislocations from the surface contact edges. Instead, we observe the formation and release of partial dislocations, directly from the apex of the pyramid. The main qualitative difference with the 20.01 nm case is then the formation of only one pyramidal structure on top and bottom surfaces.

Compressing a smaller 4.01 nm nanosphere also leads to a qualitatively different behavior. In fact, no pyramidal structure is obtained during compression in the case. When δ is equal to 3.4 Å (9.3%), single partial dislocations nucleate from the contact edges of only one surface, and interact together to form one stair-rod dislocation, which soon dissociates into two Shockley partial dislocations. These dislocations glide to the opposite side of the surface, until they escape from the nanoparticle. Then, the same mechanism reproduces from the opposite surface.

Focussing first on the possible relation between nanoparticle size and plasticity mechanisms, an apparent size dependence could be observed regarding the formation of pyramidal structures composed of stair-rod dislocations. In fact, for a large nanoparticle (20.01 nm), two pyramids are sequentially formed on both contact surfaces. Only the first one is formed for the intermediate size (8.00 nm), and none for the smallest system (4.01 nm). However, the situation is more complex and strongly depends on the fine structure of the contact surfaces. To prove it, we investigated the compression of a 20.17 nm nanoparticle. Since it is only slightly larger than the 20.01 nm nanosphere, the formation of two pyramidal structures is expected. Instead, our simulations revealed the formation of only one pyramid from both contact surfaces. This surprising result can be understood by examining the contact surface area (Table 1). Hence, we define λ_1 and λ_2 as the separations along [1 0 1] between the contact surface edges (Fig. 5b and c). In the case of the 20.17 nm nanoparticle, for which the contact surface area is much larger, the analysis of the atomic configurations after the formation of the first pyramid reveals that a second pyramid started to form, but that gliding partial dislocations interacted with the stair-rod dislocations of the first pyramidal structure. This interaction, due to the too short separation between first and second contact surface edges, inhibited the formation of a second pyramid. Instead, for the 20.01 nm nanoparticle, the larger value of λ_1 allows for the formation of two successive pyramids. This argument also explains why there is only a single pyramidal structure for the 8.00 nm nanoparticle ($\lambda_1 = 3\sqrt{2}a_0/4$), and no formation of a third pyramidal structure in all cases since λ_2 is small for the sizes considered here. Additionally, one could say that a short separation between steps defining the contact surface edges does not allow for an efficient stress concentration, and new dislocations nucleate more easily from another high stress region like the pyramidal apex (Fig. 5).

Finally, the absence of pyramidal formation in the case of the smallest 4.01 nm nanosphere is probably due to a different factor. In fact, because of the small size, there is a strong interaction between the first nucleated dislocations and the opposite side of the nanosphere. Partial dislocations are attracted to the opposite surface, and propagate through the nanoparticle thus preventing the formation of stair-rod dislocations. The consequences of a small available volume for dislocation propagation have already been suggested in the case of nickel nanowires [31].

We focus now on the relation between the nanoparticle size and the yield stress. The later is usually defined at the onset of plastic deformation, then often related to the nucleation of the first dislocation in the case of defect-free nanostructures. However, our simulations revealed that the first nucleated dislocations, leading to the pyramidal-like structure formation, will spontaneously retract to the surface if the load is removed. This 'pseudo-elastic'

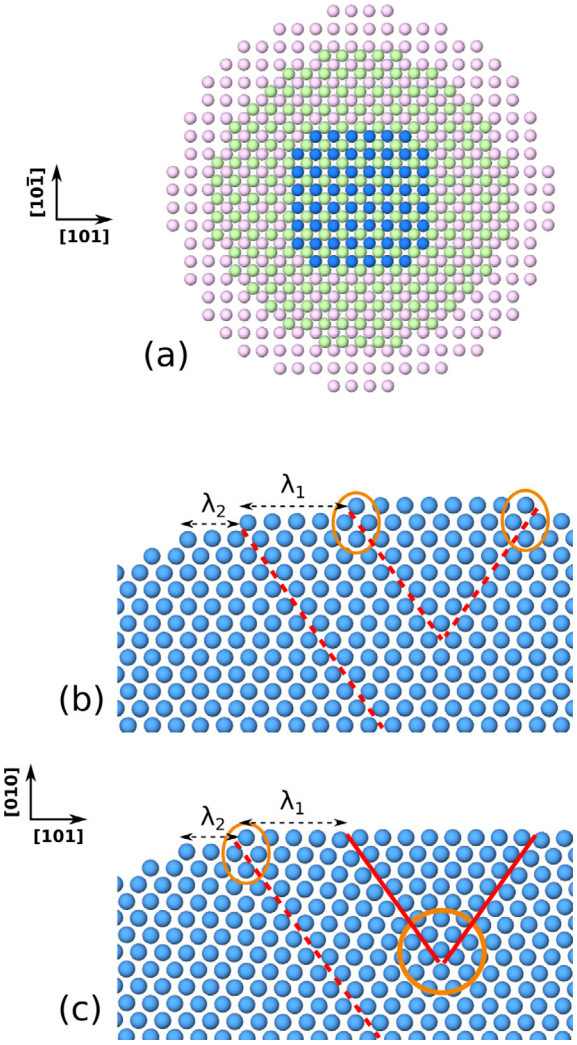

Fig. 5. (a) Top view (along [0 1 0]) of the 20.01 nm nanosphere. Only the three first atomic layers are represented with different colors for clarity. (b, c) Side view of the same nanosphere, before compression (b) and after nucleation of the first pyramidal structure (c). The red lines show {1 1 1} planes, and the orange ellipsis the regions where the atomic stresses are the largest during compression. λ_1 (λ_2) is the distance along the [1 0 1] axis, between the first and second (second and third) layer edges. (For interpretation of the references to colour in this figure legend, the reader is referred to the web version of this article.)

behavior brings an additional difficulty in defining the yield stress. Therefore we determined two yield stresses here, one associated to the nucleation of the very first dislocation (σ_1^c), and a second one corresponding to the nucleation of dislocations associated with the dissociation of the stair-rod dislocations forming the pyramid edges (σ_2^c). Note that in the case of a 4 nm nanoparticles, there is only one value since no pyramidal-like formation is obtained. The Table 1 reports several quantities corresponding to the very first nucleated dislocation (load, contact surface area and contact stress σ_1^c) as well as σ_2^c. One can see that σ_1^c is almost constant for the three first systems, but significantly lower for the fourth. Since the main difference between the 20.01 nm and 20.17 nm nanoparticles is the different contact surface, we conclude that the size effect, if any for the size range investigated here, is negligible compared to the atomic structure of the contact surfaces. Since we found that dislocations leading to pyramid-like structures tend to retract to the closest surface upon unloading, the variation of σ_2^c as a function of nanosphere radius is also analyzed. It is also clear from Table 1 that there is not a clear dependence between the system size and σ_2^c. A similar conclusion has been drawn in the case of the nanoindentation of nickel nanowires [31].

As noted in the introduction, there have been few theoretical works investigating a possible size effect for the mechanical properties of metallic nanoparticles. In one of these, Mordehai and coworkers proposed a model for the nucleation of dislocation at the onset of plasticity [32,33], where the maximum stress depends on the nanoparticle size and the stress decreases from the surface to the nanoparticle interior according to an inverse power law and an exponent of about 0.66. We then tried to apply this model to our results. We found that (i) the maximum shear stress occurs in the vicinity of the step, but that the magnitude is about 4 GPa for all nanoparticle sizes, in disagreement with this model (ii) the stress decreases from the surface to the nanoparticle center, but fitting this variation with an inverse power-law results in a low correlation coefficient and an exponent equal to 0.47. Therefore it seems that this nucleation model does not apply to the case of nanospheres.

4. Conclusions

In this work, MD simulations were performed to study the compressive deformation of aluminum spherical nanoparticles oriented along ⟨0 0 1⟩. In particular, we aimed at investigating the influence of size on the plasticity mechanisms and yield stress. It appears that in any cases the initial plastic deformation occurs by nucleation of Shockley partial dislocations from the contact edge top and bottom surfaces. For large enough nanoparticles (i.e. with 8.00 nm diameter and above), the interaction of partial dislocations on {1 1 1} planes forms a pyramidal structures on top and bottom surfaces. Depending on the contact surface area, a second larger pyramid can form outside the first one upon further compression for the largest nanospheres considered here (about 20 nm diameter). Unloading the nanospheres lead to the disappearance of these pyramid-like structures, the partial dislocations retracting towards the nearest surface. This stage then appears to be pseudo-elastic. An irreversible plastic deformation is achieved only when dislocations are nucleated from the pyramid (or from the surface in the case of the 4 nm nanosphere). They propagate through the nanoparticle, being sometimes slowed down during a short time because of dislocation interactions, until they escape from the opposite surface. We found that there is no well defined size effect for the nanoparticles investigated here, for both the mechanisms and the yield stress. In fact, our results indicate that this is rather the atomic structure of the contact surface that controls the initiation and propagation of plasticity. The importance of surface steps has already been emphasized in the elastic regime [34] and for friction [35]. Our work shows that they are also determinant in the dislocation-mediated plastic regime. One possible explanation for the absence of size-effect in this study might be related to the narrow size range of the investigated systems. Another is the idealized nature of our simulations. In fact, here we simulated the perfectly ⟨0 0 1⟩ oriented compression of spherical metallic nanoparticles with bare surfaces, at low temperature, as a first approach to understand the mechanical properties of these systems. Nevertheless, such ideal conditions are rarely encountered in real experiments, usually performed at ambiant temperature, no specific orientations, and with nanoparticles covered with an oxide layer. The pyramidal-like structures are clearly a direct consequence of the ⟨0 0 1⟩ orientation. A small misorientation and the influence of temperature are expected to delay their formation, but not totally suppress it. Ultimately, to bridge the gap between experiments and theory, a large set of additional calculations would be necessary, especially to build a statistics for different orientations and temperatures. Taking into account the

coating layer is a more difficult task, but would bring essential information for a better comprehension of the mechanical properties of nanoparticles.

Acknowledgments

Computations have been performed on the supercomputer facilities at the Mésocentre de calcul SPIN hosted by the Université de Poitiers.

References

[1] W.W. Gerberich, W.M. Mook, C.R. Perrey, C.B. Carter, M.I. Baskes, R. Mukherjee, A. Gidwani, J. Heberlein, P.H. McMurry, S.L. Girshick, Superhard silicon nanospheres, J. Mech. Phys. Solids 51 (6) (2003) 979–992.
[2] Haiyi Liang, Moneesh Upmanyu, Hanchen Huang, Size-dependent elasticity of nanowires: nonlinear effects, Phys. Rev. B 71 (24) (2005) 241403.
[3] Matthew T. McDowell, Austin M. Leach, Ken Gall, On the elastic modulus of metallic nanowires, Nano Lett. 8 (11) (2008) 3613–3618.
[4] Oliver Kraft, Patric A. Gruber, Reiner Mönig, Daniel Weygand, Plasticity in confined dimensions, Annu. Rev. Mater. Res. 40 (2010) 293–317.
[5] Dan Mordehai, Michael Kazakevich, David J. Srolovitz, Eugen Rabkin, Nanoindentation size effect in single-crystal nanoparticles and thin films: a comparative experimental and simulation study, Acta Mater. 59 (6) (2011) 2309–2321.
[6] Julia R. Greer, Jeff Th.M. De Hosson, Plasticity in small-sized metallic systems: intrinsic versus extrinsic size effect, Prog. Mater. Sci. 56 (6) (2011) 654–724.
[7] Dan Guo, Guoxin Xie, Jianbin Luo, Mechanical properties of nanoparticles: basics and applications, J. Phys. D: Appl. Phys. 47 (1) (2014) 013001.
[8] S.G. Corcoran, R.J. Colton, E.T. Lilleodden, W.W. Gerberich, Anomalous plastic deformation at surfaces: nanoindentation of gold single crystals, Phys. Rev. B 55 (24) (1997) R16057.
[9] W.M. Mook, J.D. Nowak, C.R. Perrey, C.B. Carter, R. Mukherjee, S.L. Girshick, P.H. McMurry, W.W. Gerberich, Compressive stress effects on nanoparticle modulus and fracture, Phys. Rev. B 75 (21) (2007) 214112.
[10] William W. Gerberich, William M. Mook, Megan J. Cordill, C. Barry Carter, Christopher R. Perrey, Joachim V. Heberlein, Steven L. Girshick, Reverse plasticity in single crystal silicon nanospheres, Int. J. Plast. 21 (12) (2005) 2391–2405.
[11] Julia Deneen, William M. Mook, Andrew Minor, William W. Gerberich, C. Barry Carter, In situ deformation of silicon nanospheres, J. Mater. Sci. 41 (14) (2006) 4477–4483.
[12] L.M. Hale, X. Zhou, J.A. Zimmerman, N.R. Moody, R. Ballarini, W.W. Gerberich, Phase transformations, dislocations and hardening behavior in uniaxially compressed silicon nanospheres, Comput. Mater. Sci. 50 (5) (2011) 1651–1660.
[13] L.M. Hale, D.-B. Zhang, X. Zhou, J.A. Zimmerman, N.R. Moody, T. Dumitrica, R. Ballarini, W.W. Gerberich, Dislocation morphology and nucleation within compressed Si nanospheres: a molecular dynamics study, Comput. Mater. Sci. 54 (2012) 280–286.
[14] Roman Kositski, Dan Mordehai, Depinning-controlled plastic deformation during nanoindentation of {BCC} iron thin films and nanoparticles, Acta Mater. 90 (2015) 370–379.
[15] J. Amodeo, C. Begau, E. Bitzek, Atomistic simulations of compression tests on ni3al nanocubes, Mater. Res. Lett. 2 (3) (2014) 140–145.
[16] Koren Shreiber, Dan Mordehai, Dislocation-nucleation-controlled deformation of ni3al nanocubes in molecular dynamics simulations, Model. Simul. Mater. Sci. Eng. 23 (8) (2015) 085004.
[17] A. Prakash, J. Guénolé, J. Wang, J. Muller, E. Spiecker, M.J. Mills, I. Povstugar, P. Choi, D. Raabe, E. Bitzek, Atom probe informed simulations of dislocation–precipitate interactions reveal the importance of local interface curvature, Acta Mater. 92 (2015) 33–45.
[18] Jian-Jun Bian, Gang-Feng Wang, Atomistic deformation mechanisms in copper nanoparticles, J. Comput. Theor. Nanosci. 10 (9) (2013) 2299–2303.
[19] Steve Plimpton, Fast parallel algorithms for short-range molecular dynamics, J. Comput. Phys. 117 (1) (1995) 1–19.
[20] Y. Mishin, D. Farkas, M.J. Mehl, D.A. Papaconstantopoulos, Interatomic potentials for monoatomic metals from experimental data and ab initio calculations, Phys. Rev. B 59 (5) (1999) 3393.
[21] Yu. Mishin, M.J. Mehl, D.A. Papaconstantopoulos, A.F. Voter, J.D. Kress, Structural stability and lattice defects in copper: ab initio, tight-binding, and embedded-atom calculations, Phys. Rev. B 63 (22) (2001) 224106.
[22] S. Brochard, P. Hirel, L. Pizzagalli, J. Godet, Elastic limit for surface step dislocation nucleation in face-centered cubic metals: temperature and step height dependence, Acta Mater. 58 (12) (2010) 4182–4190.
[23] Pierre Hirel, Sandrine Brochard, Laurent Pizzagalli, Pierre Beauchamp, Effects of temperature and surface step on the incipient plasticity in strained aluminium studied by atomistic simulations, Scripta Mater. 57 (12) (2007) 1141–1144.
[24] Douglas E. Spearot, Karl I. Jacob, David L. McDowell, Dislocation nucleation from bicrystal interfaces with dissociated structure, Int. J. Plast. 23 (1) (2007) 143–160.
[25] William G. Hoover, Canonical dynamics: equilibrium phase-space distributions, Phys. Rev. A 31 (3) (1985) 1695.
[26] Maxim Vergeles, Amos Maritan, Joel Koplik, Jayanth R. Banavar, Adhesion of solids, Phys. Rev. E 56 (3) (1997) 2626.
[27] Ju Li, Atomeye: an efficient atomistic configuration viewer, Model. Simul. Mater. Sci. Eng. 11 (2) (2003) 173.
[28] Cynthia L. Kelchner, S.J. Plimpton, J.C. Hamilton, Dislocation nucleation and defect structure during surface indentation, Phys. Rev. B 58 (17) (1998) 11085.
[29] Alexander Stukowski, Visualization and analysis of atomistic simulation data with ovito–the open visualization tool, Model. Simul. Mater. Sci. Eng. 18 (1) (2010) 015012.
[30] Amy Henderson Squillacote, The paraview guide: a parallel visualization application, Kitware inc., 2007. Technical report, ISBN: 1-930934-21-1.
[31] V. Dupont, F. Sansoz, Molecular dynamics study of crystal plasticity during nanoindentation in ni nanowires, J. Mater. Res. 24 (3) (2009) 948.
[32] Dan Mordehai, Seok-Woo Lee, Björn Backes, David J. Srolovitz, William D. Nix, Eugen Rabkin, Size effect in compression of single-crystal gold microparticles, Acta Mater. 59 (13) (2011) 5202–5215.
[33] Yosi Feruz, Dan Mordehai, Towards a universal size-dependent strength of face-centered cubic nanoparticles, Acta Mater. 103 (2016) 433–441.
[34] Gangfeng Wang, Jianjun Bian, Juan Feng, Xiqiao Feng, Compressive behavior of crystalline nanoparticles with atomic-scale surface steps, Mater. Res. Express 2 (1) (2015) 015006.
[35] B. Luan, M.O. Robbins, The breakdown of continuum models for mechanical contacts, Nature 435 (2005) 929.